MEASURING CMB POLARIZATION WITH QUIET: THE Q/U IMAGING EXPERIMENT

LAURA NEWBURGH FOR THE QUIET COLLABORATION

Columbia University, 550 W 120th St., New York, NY 10027, USA
newburgh@phys.columbia.edu

Phase I of the Q/U Imaging ExperimenT (QUIET) measures the Cosmic Microwave Background polarization anisotropy spectrum at angular scales $25 \lesssim \ell \lesssim 1000$. QUIET has deployed two independent receiver arrays. The 40-GHz array took data between October 2008 and June 2009. The 90-GHz array was deployed in June 2009 and observations are ongoing. Described in this proceeding are the instrument, analysis procedures, and expected science reach for the QUIET Phase I arrays. We also briefly discuss the science forecasts for QUIET Phase II in which arrays roughly an order-of-magnitude larger will be deployed.

Keywords: telescopes, cosmic microwave background, gravitational waves, millimeter wave, cosmology: observations, cosmology: inflation, instrumentation:polarimeters

1. Science Motivation

Anisotropies present in the polarized Cosmic Microwave Background (CMB) can be used to constrain models describing the physics in the very early Universe. Maps of the polarized CMB can be decomposed into E-mode (curl-free) and B-mode (divergence-free) components. Measurements of the E-mode anisotropy spectrum will break degeneracies between cosmological parameters when used in conjunction with the CMB temperature anisotropy spectrum. Many inflation models predict that gravity waves generated during inflation will leave a unique signature in the B-mode polarization spectrum near angular scales of $\ell \simeq 100$. In those models, measurement of the ratio, r , of the amplitude of the B- to E-mode spectrum will yield the energy-scale of inflation. Placing upper limits of $r < 0.01$ can rule out large classes of inflationary models.

2. QUIET Instrument and Observations

2.1. *QUIET Instrument*

The QUIET instrument consists of two independent receivers. Each receiver comprises a hexagonal array of High Electron Mobility Transistor (HEMT)-based polarimeters: one array operates at 40 GHz (Q band) with 19 polarimeters and the other at 90 GHz (W band) with 90 polarimeters. The Q-band receiver dedicates one pair of polarimeters (hereafter: TT channels) to the observation of the CMB temperature anisotropy spectrum. The W-band receiver has three pairs of TT channels. The external optics are a 1.4-m Cross-Dragone reflector design with FWHM beamwidth of 27 arcmin at Q-band and 12 arcmin at W-band. Salient characteristics of QUIET Phase I are shown in Table 1.

As shown in a cut-away view of the W-band cryostat (Fig. 1), light enters the

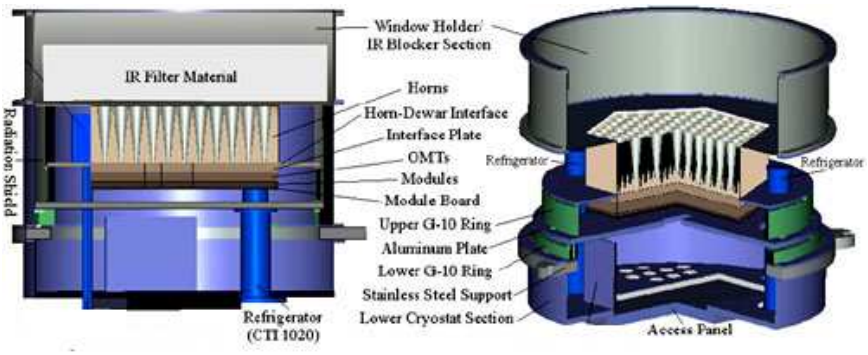

Fig. 1. Cut-away of the original design of the W-band cryostat, internal components are labeled accordingly. The vacuum window is an anti-reflection coated polyethylene sheet. The W-band cryostat has a diameter of 71 cm and length of 66 cm. The Q-band cryostat has the same diameter and length of 71 cm.

cryostat through an expanded-Teflon coated high-density polyethylene window and impinges upon a set of corrugated feedhorns. The feedhorn arrays are constructed from a series of thick, corrugated plates machined and diffusion bonded together. Detailed measurements of the return loss and beam characteristics of these horns show that they perform well in comparison to a electroformed horn of the same design, while the combined cost of machining and diffusion bonding these arrays is at least an order of magnitude less than the cost of producing the same number of electroformed feedhorns. After the feedhorns, the light is then directed into septum polarizer OMTs, which separate radiation into left- and right-circularly polarized components (Ref. 1), and is guided into the two input legs of a QUIET polarimeter. The signal is amplified, phase-modulated, and read out in each QUIET polarimeter (discussed below). The active components inside each polarimeter are biased by electronics housed in a thermally-regulated enclosure. Receiver and telescope encoder data are read at 100 Hz, the housekeeping and weather data at 1 Hz.

Table 1. QUIET Phase I instrument and observations.

Frequencies	40 / 90 GHz
# of Detectors	17 Polarization and 2 TT / 84 Polarization and 6 TT
Telescope	Cross-Dragone
Angular Resolution	27 arcmin / 12 arcmin
Field Centers	181°/-39°, 78°/-39°, 12°/-48°, 341°/-36° (J2000 RA/Dec)
Field Size	15° × 15°
Instrument Sensitivity	$64\mu\mathrm{K}\sqrt{s}$ / $57\mu\mathrm{K}\sqrt{s}$

WMAP, DASI, CBI, and CAPMAP (Refs. 2, 3, 4, 5) used HEMT-based polarimeters, but QUIET employs a revolutionary compact-profile design (Ref. 6) suitable for arrays. The QUIET polarimeter design replaces waveguide-block components and connections with strip-line coupled devices, producing modules with a

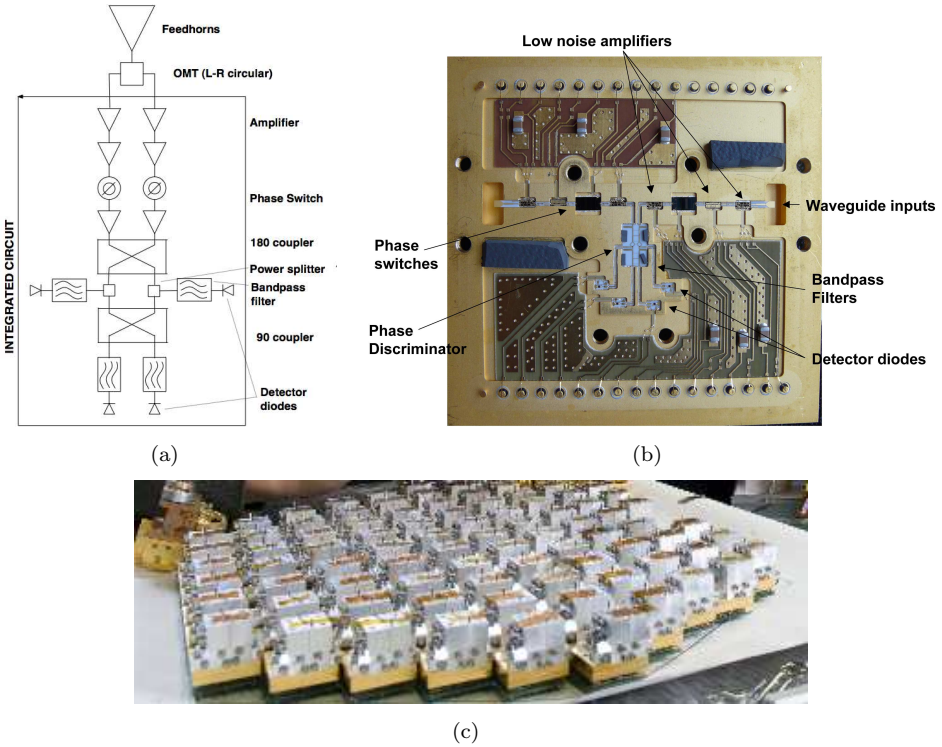

Fig. 2. *a:* Schematic of signal processing components in a QUIET polarimeter. *b:* Internal components of a Q-band polarimeter. *c:* W-band array of polarimeters.

footprint of 2.5cm×2.5cm (W-band) and 5cm×5cm (Q-band). A schematic of the signal processing in a single QUIET polarimeter is shown in Fig. 2(a) and a photograph of a Q-band polarimeter is shown in Fig. 2(b) with relevant components labeled. Radiation from the septum polarizers is incident on a set of waveguide probes, one on each leg of the polarimeter. The signal on each leg is amplified independently through three low-noise amplification stages, and is separately phase switched: one leg at 4 kHz, the other at 50 Hz. The signals enter a 180° hybrid coupler and the outputs from the coupler are split. One half of each leg is measured in a "Q" detector diode, while the other half continues into a 90° hybrid coupler and is detected in a "U" detector diode.

Each diode is differenced at the phase-switching rate. Differencing the signal measured on the "Q" detector diodes at 4 kHz corresponds to measuring the Stokes ±Q polarization parameters. The ±U polarization parameters are found by differencing the second pair of detector diodes. Summing instead of differencing yields a measurement of total intensity. High frequency differencing limits contributions from more slowly varying noise and offsets, resulting in data power spectra with $1/f$ knees considerably below the telescope scan frequencies ($\simeq$ 0.1 Hz). QUIET employs an additional differencing at 50 Hz to remove systematic contamination

arising from, for example, transmission imbalances between the polarimeter legs and is accomplished without loss of signal. Electronic phase modulation has helped to keep the optical chain simple and QUIET free from systematics resulting from polarization modulation via optical components. The W-band array is pictured in Fig. 2(c) - with 90 polarimeters, it is the largest HEMT-based array yet deployed.

2.2. *QUIET Observations*

QUIET observations are performed from the Chajnantor Test Facility (CTF). The CTF is located at an altitude of 5080m in the Atacama Desert in northern Chile. Between July and September 2008, the Q-band receiver was deployed to the CTF and calibration and commissioning observations were performed. Science data were collected between October 2008 and June 2009. The Q-band receiver was removed and replaced by the W-band receiver in June 2009 and observations are currently underway. We logged over 3000 hours of CMB data during the Q-band observing season. We have collected more than 3000 hours of W-band data and anticipate collecting 4500 additional hours by the end of December 2010.

The telescope mount can rotate in three independent axes (azimuth, elevation, and boresight, or 'deck', rotation). QUIET observes at deck angles {30°, 75°, 120°, 165°} over the season; stepping the deck angle by 45° rotates the Stokes Q into Stokes U parameters.

We scan four CMB patches (2a, 4a, 6a, 7b) and two Galactic patches (Gb, Gc), each covering 15° × 15°. The QUIET patch coordinates are given in Table 1 and shown in Fig. 3. QUIET patches were selected for their low synchrotron emission as measured by WMAP and because they remain at least 30° from the Sun and Moon throughout the year, allowing uninterrupted observations throughout the season.

We employ a fixed-elevation, azimuth-scanning technique: a patch is scanned in azimuth as it drifts through the beam, which generally takes ≃1.5 hours. The telescope then re-tracks the patch and begins another scan. By scanning at constant elevation for each patch scan, we observe through a constant column density of atmosphere and ensure a stable atmospheric contribution (during periods of good

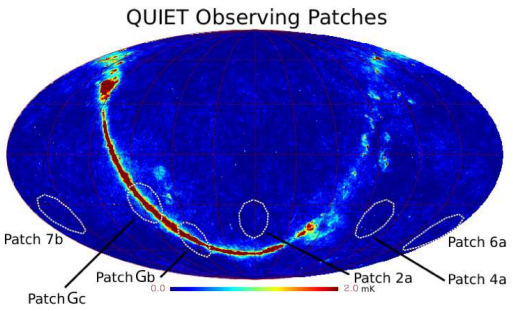

Fig. 3. QUIET sky patches (circles), plotted over the WMAP Q-band temperature map (Ref. 10), range from 0 to 2 mK.

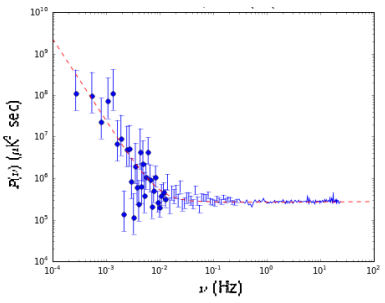

Fig. 4. The Fourier transform of a typical QUIET scan for a single detector diode of one polarimeter.

weather) to a given observation.

A Fourier transform of a typical data stream from one diode during a 1.5-hour scan of patch 6a is shown in Fig. 4. High-pass and low-pass filters are applied during data analysis, so the high frequency noise and $1/f$ contributions to the noise spectrum are removed. QUIET operates the telescope at its maximum slew rate of 6°/sec, resulting in scan frequencies $\simeq 0.1$ Hz. These are significantly higher than typical instrument knee frequencies ($\simeq$0.02 Hz), such that we scan in the white-noise regime of the detectors.

2.3. *Calibration and Pointing*

We dedicate $\simeq$10% of our observing time to calibration measurements. The calibration sources are described below, and the Q-band calibration scheme is summarized in Table 2.

- **Tau A** Tau A is one of our primary absolute calibrators. The polarized flux of Tau A is measured at Q-band by WMAP within $\pm$2.7% (Ref. 7). Extrapolating to our polarimeter central frequencies gives absolute reponsivity within 7% for any measurement.
- **The Moon** We use the Moon both as an absolute and relative calibrator. Using a model of polarized emission from the Moon, we can determine the absolute polarimeter angles within $\pm 2^\circ$. These full-array scans also provide a measurement of relative responsivities between the central polarimter (which has frequent absolute responsivity measured from Tau A) and the other polarimeters.
- **Mini Sky-dips** We perform mini sky-dips once per patch scan (once per $\simeq$1.5 hours). Each mini sky-dip consists of nodding the telescope in elevation by a few degrees causing the instrument to look through different air masses. The intensity channels of the polarimeters will measure the resulting change in atmospheric temperature. Using the statistical power from the large number of mini-sky-dips performed throughout the season we can investigate a variety of instrument characteristics, including the variation of reponsivity with respect to amplifier-bias board temperature.
- **Wire grid polarizer** At the end of the Q-band season, we performed one measurement with a wire-grid polarizer, which polarizes incoming radiation and results in a polarized signal of a few Kelvin. We placed the polarizer on the front face of the cryostat and rotated the grid around the boresight, the modulated polarized signal is then measured by the polarimeters. In addition, bias voltages for the W-band array were optimized for signal-to-noise using this polarized signal.
- **Jupiter, RCW38, and Venus** Jupiter, RCW38, and Venus are used as calibrators for the TT channels. We cannot use Jupiter as a polarization calibrator due to a combination of its low polarization flux, our beam size, and our sensitivity.

We use Moon and Patch Gc observations with all polarimeters and Jupiter measurements with the TT channels for pointing. The Jupiter observations are particularly useful for pointing because Jupiter is not extended at our resolution, and because the TT channels are located $\simeq 4^\circ$ away from the boresight, providing a larger lever

arm for determining our pointing accuracy. Pointing measurements were performed once every two weeks with an optical camera at the end of the Q-band season.

Table 2. QUIET calibration plan.

Source	**Schedule**	**Calibration**
Tau A, central polarimeter	Once/two days	Beam size and ellipticity, absolute polarimeter responsivity, absolute polarimeter angles
Tau A, off-center polarimeters	Once/season	Absolute polarimeter responsivity, absolute polarimeter angles
Moon (full array scan)	Once/week	Relative polarimeter responsivity between polarimeters, pointing, leakage, absolute polarimeter angles
Jupiter, Venus, RCW38 (TT channels)	Once/week	Absolute TT responsivity, pointing, beam size and beam ellipticity
Sky dip	Once/scan	Relative TT and polarimeter responsivity, leakage monitoring
Polarized wire grid	Once/season	Relative polarimeter responsivity, relative polarimeter angles

Table 3. Preliminary calibration precision for QUIET Phase I.

	Precision	**Typical Value**	**Calibrators**
Beam			Jupiter, Tau A
Size (FWHM)	<0.1 arcmin	27/12 arcmin (Q/W)	
Ellipticity	–	<1.5%	
Pointing	4 arcmin	–	Moon, Jupiter, Patch Gc
Responsivity			
Polarization	7%	2 mV/K	Mini-sky-dips, Tau A, the Moon, polarizing grid
Intensity	5%	2 mV/K	Jupiter, Venus, RCW38
Polarization Angle	$\pm 2^\circ$	–	Mini-sky-dips, the Moon, Tau A, polarization grid
I $\rightarrow$ Q/U Leakage	$\pm$0.5dB	-20dB / -27dB (Q/U)	Skydips, the Moon, Tau A
Correlated Noise	$\pm$0.5%	30 %	Constant elevation CMB scan

Table 3 shows the precision to which we have characterized the instrument, to date. Relative responsivities from mini-sky-dips, the Moon, and Tau A agree to 6% which translates to a $\simeq$2% accuracy in the power spectrum uncertainty. The polarized angles computed from measurements of the Moon, Tau A, and the polarization grid are consistent with each other.

Two systematic uncertainties of particular interest are correlated noise and temperature -to-polarization (I-to-Q/U) leakage. The correlated noise between "Q" and "U" diodes in a single polarimeter can be as high as 30%. The correlation coefficients are computed to within 1% per 1.5-hour map scan and accounted for in the analysis. I-to-Q/U leakage from the Q-band polarimeters is well calibrated using the Moon, TauA, and skydip measurements. The mechanism generating this leakage is understood as a waveguide mode in the septum polarizer which would normally be suppressed by an optimized choice of septum polarizer bandwidth and central frequency (this choice will be implemented in QUIET Phase II). The leakage value

is constant through the season and suppressed by our scan strategy, which includes sky rotations and deck rotations. We have demonstrated effective removal of this leakage in our map-making stage, and its impact on the phase I science goals is negligible (discussed in future papers, in preparation). Simulations of cross-polar leakage from optics show this to be constrained to <0.3%. All instrument characteristics are consistent with the phase I science goals for the Q-band array.

3. QUIET Data Analysis and Science Prospects

Data reduction and analysis are performed on each patch using two independent pipelines, one employing maximum-likelihood map-making and power spectrum estimation (Ref. 11), and one a Pseudo-C_ℓ estimator (Ref. 12).

3.1. *Data Selection*

We evaluate the quality of our data to decide which parts can be used for science analysis. The baseline data selection (removing dead detector diodes, engineering tests during the season, and glitching) is common between the two pipelines, but each pipeline has developed independent criteria based on analysis of the time-ordered data stream, spectral information, and map-based tests. We have found the percentage of data kept is similar between the two pipelines and preliminary data selection indicates an acceptance efficiency of $\simeq$60%. Studies are ongoing for additional cuts, including analyzing null-test results, discussed in the next section.

3.2. *Null Tests*

After preliminary data selection, the resulting data set is subjected to a set of null tests. In a null test, the pipeline divides the data in half, makes a map of each half, subtracts one map from the other, and computes the resulting map and its power spectrum. The null test is successful if the signal has been fully removed and the spectrum computed is null within noise. A non-null result indicates the presence of signal in the resulting map, which could be from instrumental systematic errors or poor quality data (weather, etc).

We currently have a suite of over 40 null tests which we categorize as temporal (eg. first/second halves of the season, night vs day), telescope (eg. various deck angles and elevation values against others, sidelobe elevation), and receiver (eg. inner polarimeters vs outer polarimeters, high vs low temperature-to-polarization leakage polarimeters), each designed to explore immunity to a certain systematic error. Both pipelines are using a blind analysis technique such that each set in the the suite of null tests must be consistent with no systematic effects before the power spectrum of the signal is computed. Each of the $\sim$40 null tests contains ten EE- and ten BB-power-spectrum points, giving a total of 800 points that should be consistent with zero.

3.3. *Preliminary Map of a Galactic Patch*

A WMAP map of QUIET Patch Gb with 5 years of data is shown in Fig. 5(a) (this represents $\simeq$ 1% of their sky coverage), and a map of the same patch with

≃100 hours of QUIET Q-band data generated by the maximum-likelihood mapping algorithm is shown in Fig. 5(b). The QUIET map is shown with pixel size adjusted to maintain constant noise across the map, and the pixelization was maintained for ease of comparison for the WMAP map. The source in the center of the QUIET maps is also present in the WMAP map, but with much greater signal to noise in the QUIET map.

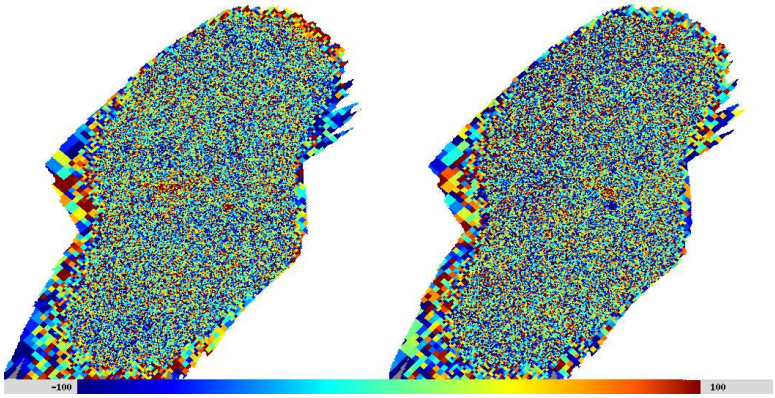

(a)

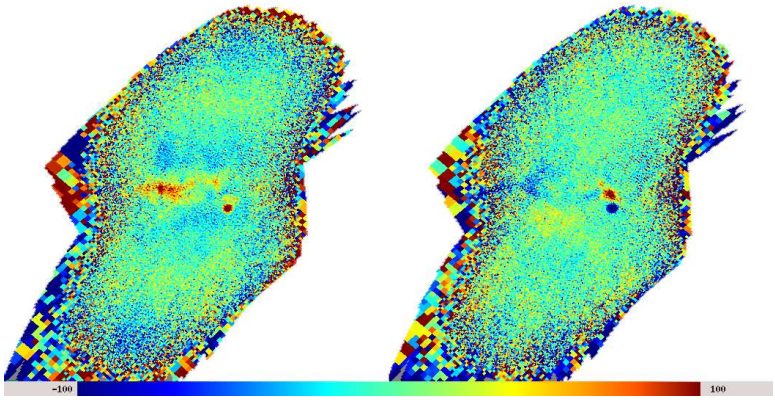

(b)

Fig. 5. *(a)* WMAP polarized map of QUIET Patch Gb. *(b)* Same patch, with QUIET Q-band data. Left panel is Stokes Q, right panel is Stokes U parameters. Units are in μK.

3.4. *Science Prospects*

On-sky measurements of sensitivity give values of 64±8 $\mu\mathrm{K}\sqrt{s}$ for the Q-band array, and 57±14 $\mu\mathrm{K}\sqrt{s}$ for the W-band array. The projected E-mode polarization anisotropy spectrum for each array is shown in Fig. 6, with the measurements from BICEP and QUaD (Refs. 8, 9). Over the range $50 < \ell < 1000$, we will significantly

improve measurement of the EE polarization power spectrum. Further, QUIET will make the most sensitive maps of synchrotron emission in a relatively foreground-free region of the sky (Ref. 13).

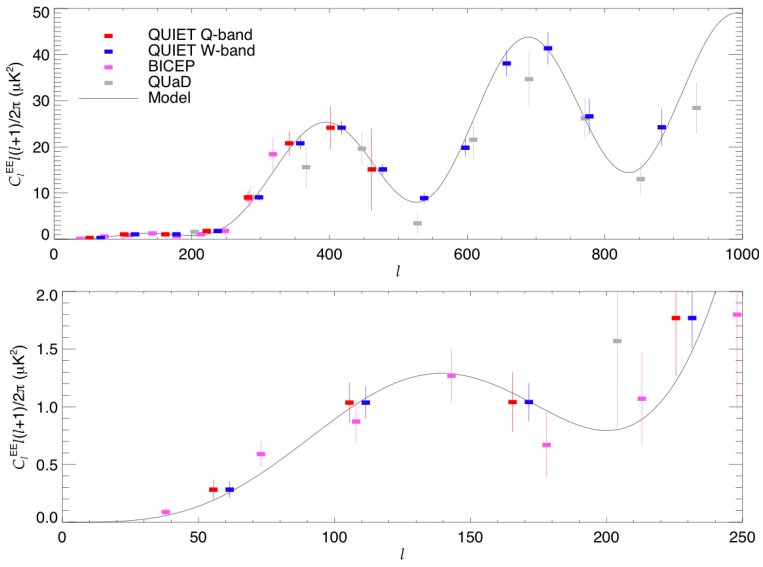

Fig. 6. *Upper* Forecast precision of QUIET Phase I measurements assuming ≃3000 hours of Q-band data and ≃4500 hours of W-band data compared with results from BICEP (Ref. 8) and QUaD (Ref. 9). *Lower* Same for smaller range of ℓ <250.

4. QUIET Phase II

QUIET Phase II will consist of three separate telescopes with four cryostats. Three cryostats will house identical W-band arrays of 499 polarimeters at 90 GHz, 36 polarimeters in each array will be dedicated TT assemblies. The fourth cryostat will be a hybrid of 61 Q-band polarimeters at 40 GHz and 18 Ka-band polarimeters at 32 GHz, with six and two polarimeters dedicated to TT assemblies, respectively.

The increased sensitivity of Phase II and larger primary mirror (2 m diameter mirrors compared to 1.4 m) will allow measurements of the CMB polarization anisotropy spectrum to significantly higher resolution. The projected EE- and BB-polarization anisotropy power spectra for Phase II are shown in Fig. 7. QUIET Phase II expects to constrain the tensor-to-scalar ratio r to 0.01.

5. Conclusion

QUIET has successfully fielded two HEMT-based arrays for its Phase I stage. Observing has been completed with the Q-band array and is ongoing for the W-band array. Data analysis is underway and the data quality is good. We expect to place constraints on the tensor-to-scalar ratio which are competitive with the current limits. The planned QUIET Phase II, with over 1600 QUIET polarimeters, will be capable of constraining the tensor-to-scalar ratio to $r \simeq 0.01$.

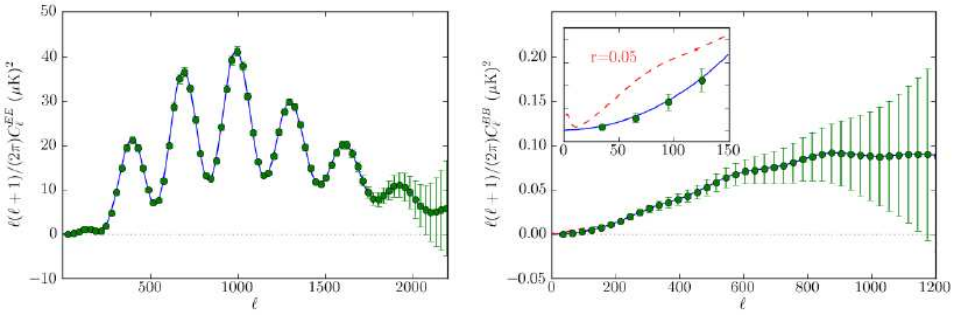

Fig. 7. *Left* Projected EE spectrum of QUIET Phase II W- band arrays.
Right Projected BB limits for QUIET Phase II W-band arrays, the inset shows the expected sensitivity near $\ell \simeq 100$ compared to a spectrum with tensor-to-scalar ratio of $r = 0.05$.

Acknowledgments

Support for the QUIET instrument and operations comes through the NSF cooperative agreement AST-0506648. Support also provided by AST-04-49809, DE-AC02-05CH11231, JSPS KAKENHI (A) 20244041, and by the Strategic Alliance for the Implementation of New Technologies (SAINT). Some work presented was performed on the Joint Fermilab - KICP Supercomputing Cluster, supported by grants from Fermilab, Kavli Institute for Cosmological Physics, and the University of Chicago. We are particularly indebted to the engineers who maintained and operated the telescope: J. Cortes, C. Jara, F. Munoz, and C. Verdugo.

References

1. Bornemann, J., & Labay, V. A. *Ridge waveguide polarizer with finite and stepped-thickness septum*, IEEE Trans. MTT, 43, 95 (1995).
2. Jarosik, N. *et al.*, *ApJS*, **145**: 413 (2003).
3. Leitch, E. *et al.*, *Nature*, **420**:763-771 (2002).
4. Padin, S. *et al.*, *PASP*, **114**: 83-97 (2002).
5. Barkats, D. *et al.*, astro-ph/0503329v1.
6. Lawrence, Gaier and Seiffert, *Proceedings of the SPIE*, **5498**, pp. 220–331, eds. J. Zmuidzinas, W. S. Holland and S. Withington (2004).
7. Weiland, J. *et al.*, astro-ph/1001.4731v1.
8. Chiang, H. C. *et al.*, *ApJ.*, **711**:1123-1140 (2010), astro-ph/0906.1181.
9. Brown, M. L. *et al.*, *ApJ.*, **705**: 978-999 (2009), astro-ph/0906.1003.
10. Hinshaw, G. *et al.*, *ApJS.*, **180**: 225–245 (2009).
11. Eriksen, H. K. *et al.*, *ApJ.*, **676**:10 (2008), astro-ph/0709.1058.
12. Smith, K. M. and Zaldarriaga, M. *Phys.Rev.***D76**: 043001 (2007) astro-ph/0610059.
13. Dunkley, J. *et al.*, *AIP Conf. Proc.* **1141**:222-264 (2009), astro-ph/0811.3915v2.